Chapter 4

Colloidal III–V Nitride Quantum Dots

Zequn Chen, Chuli Sun, Wei Guo and Zhuo Chen

Additional information is available at the end of the chapter

http://dx.doi.org/10.5772/intechopen.70844

Abstract

Colloidal quantum dots (QDs) have attracted intense attention in both fundamental studies and practical applications. To date, the size, morphology, and composition-controlled syntheses have been successfully achieved in II–VI semiconductor nanocrystals. Recently, III-nitride semiconductor quantum dots have begun to draw significant interest due to their promising applications in solid-state lighting, lasing technologies, and optoelectronic devices. The quality of nitride nanocrystals is, however, dramatically lower than that of II–VI semiconductor nanocrystals. In this review, the recent development in the synthesis techniques and properties of colloidal III–V nitride quantum dots as well as their applications are introduced.

Keywords: colloidal synthesis, III–V nitride, quantum dots, semiconductor, optoelectronic properties

1. Introduction

Due to the uniquely tunable electronic structure and low-cost synthesis in a controllable way, colloidal quantum dots (QDs) have attracted intense attention in both fundamental studies and practical applications [1–5], such as solar cell, quantum dot light-emitting diode, and spectrometer. Usually, semiconductor quantum dot properties can be varied by their size, composition, morphology, and phase structure. To date, with the rapid development of synthesis technique, the size, morphology, and composition-controlled syntheses of colloidal quantum dots have been successfully achieved [6–9].

III–V semiconductors are crystalline binary compounds formed by combining metallic elements from group III and nonmetallic elements from group V of the periodic table [10]. In the III–V nitride, the wurtzite phase is the stable form and they have direct bandgaps ranging from 0.7 eV for InN, to 3.4 eV for GaN, and to 6.2 eV for AlN. They can combine with each other to form alloys with bandgaps value from 0.7 to 6.2 eV, covering a wide range of spectra from

INTECH
open science | open minds

© 2018 The Author(s). Licensee InTech. This chapter is distributed under the terms of the Creative Commons Attribution License (http://creativecommons.org/licenses/by/3.0), which permits unrestricted use, distribution, and reproduction in any medium, provided the original work is properly cited. CC BY

ultraviolet (UV) to infrared region, exhibiting large potential applications for electronic and optoelectronic devices.

Recently, III-nitride semiconductor (such as GaN, InN, and AlN) quantum dots (QDs) have begun to draw significant interest due to their promising applications in solid-state lighting, lasing technologies, and optoelectronic devices. The quality of nitride nanocrystals is, however, dramatically lower than that of II–VI semiconductor nanocrystals. For synthesis of III–V nitride quantum dots with uniform distribution, it is important to have a very fast nucleation and relatively slow growth process, which requires the growth unit concentration to reach high super-saturation level. However, such condition is very difficult to achieve for nitride quantum dots due to their strong covalent bonding and lack of suitable precursors. Although during the past few decades, various methods and precursors have been studied, the effective reaction with a control over group III elements and nitrogen in the solution has still remained difficult. Herein, we review the recent development in the synthesis techniques and properties of colloidal III–V nitride quantum dots as well as their applications. Meanwhile, the overview will partially involve the development and improvement of III-nitride QDs grown by vapour-phase methods. More detailed introduction of colloidal III–V nitride quantum dots, that is, GaN, InN, and their alloys, are presented in the following discussion.

1.1. Gallium nitride quantum dots

GaN is a technologically important direct semiconductor for development of short-wavelength optoelectronic devices, high-speed microwave device, and high-density integrated circuit [11–13]. Its bandgap is 3.4 eV. GaN also have chemical and radiation resistance, and is therefore being considered as a stable photocatalyst in photoelectrochemical (PEC) cells for the production of fuels [14]. Colloidal QDs made from this material are expected to comprise good thermal, chemical, and radiation stability with the excellent optical properties. Therefore, since Xie [15] group succeeded in preparing GaN nanoparticles by simple inorganic reactions at 300°C, considerable efforts have been made towards the solution-based synthesis of GaN QDs at low temperature and the understanding of optical and electronic properties. In the past 20 years, many researchers have prepared zero-dimensional (0D) GaN nanostructures by top-down approach. Various methods based on a bottom-up approach, like solvothermal methods, thermal decomposition, and so on, have been used to synthesize 0D GaN QDs. However, for the wet-chemical approach, controlling the size of 0D GaN QDs and even their optical and electrical properties remains a significant challenge.

1.2. Indium nitride quantum dots

Among III–V nitrides, indium nitride is of relatively low-thermal stability. For example, the InN thin film conducts thermal decomposition under dinitrogen desorption at 500–550°C [16]. InN is one of the least studied materials in the III–V compounds. Previously, it was believed that the fundamental bandgap of InN was 1.9 eV, until much more recent studies on higher quality films of InN have clearly shown that the true value of its direct bandgap is at 0.7 eV [17], making it a very promising compound for optoelectronic applications. Recently, with the further study of the group III nitride, the semiconductor properties of InN have attracted

http://dx.doi.org/10.5772/intechopen.70844

increasing attention. It has a good property on electron transport, making it face the huge application on high-speed electronic device due to its small-effective mass [18]. InN is also considered as an excellent material for low-cost, high-efficiency solar cell, photomask, light-emitting diodes, laser diodes, sensors, and THz radiation [19–22]. In addition, InN is considered as a promising candidate for biological imaging and in vivo medical applications because of its nontoxicity and its infrared emission in the optically transparent region of water and blood [23].

With the increasing importance on InN, how to obtain the InN with high quality is also attracting much attention. Although several synthesis methods, such as solvothermal methods [24, 25], sputtering [26], and molecular beam epitaxy (MBE) [27], were developed to prepare 0D InN QDs, more effort needs to be devoted to improve the quality of InN QDs with a controlled way.

1.3. Indium gallium nitride quantum dots

Group III nitrides have a high light-emitting efficiency due to its direct bandgap as well as high radiative transition rate. GaN and InN can form component continuous solid solution and superlattice, like InGaN. The alloy's bandgap can be tuned by controlling the ratio of GaN/InN and with the increasing composition of In, the VBM of the InGaN increases in energy almost linearly [28]. In addition, due to the quantum size effect, the bandgap of the InGaN can be further tuned by changing the size and shape of the QDs, so that these semiconductors can be used for red to ultraviolet emitting devices [29].

Unlike the synthesis methods of GaN and InN, the way to prepare InGaN quantum dots are mainly top-down approach, such as plasma-assisted molecular beam epitaxy (PA-MBE) [30], metal-organic vapour phase epitaxy (MOVPE) [31], and metal-organic chemical vapour deposition (MOCVD) [32].

There are abundant papers and books to review the development of 1D and 2D III–V nitride and other nanostructures. However, there are few reviews on the research status of the colloidal III–V nitride quantum dots. This research field is important for fundamental science and technology and is growing fast. In this review, we focus on recent progresses in the synthesis, crystal structure, and optoelectronic properties of colloidal III–V nitride quantum dots.

2. Crystal structure

There are three common crystal structures shared by the group III nitrides, namely, the wurtzite, zinc blende, and rocksalt structures. Usually, the thermodynamically stable structures are wurtzite for bulk AlN, GaN, and InN. The large difference in electronegativity between the group III and group V elements (Al = 1.18, Ga = 1.13, In = 0.99, N = 3.1) results in very strong chemical bonds within the III-nitride material system, which not only is at the origin of most of the exceptional III-nitride physical properties (listed in **Table 1**), but also greatly hinder the low-temperature solution synthesis of III–V nitrides [33]. For the growth of III–V nitride QDs, vapour deposition based on substrate is a more popular approach.

	AlN	GaN	InN
Lattice constant, a (Å)	3.112	3.189	3.545
Lattice constant, c (Å)	4.982	5.186	5.703
Thermal expansion coefficient α_a (10^{-6} K^{-1})	5.27 (20–800°C)	4.3 (17–477°C)	5.6 (280°C)
Thermal expansion coefficient α_c (10^{-6} K^{-1})	4.15 (20–800°C)	4.0 (20–800°C)	3.8 (280°C)
Electron effective mass, m_e (m_0)		0.2	0.11
Hole effective mass, m_h (m_0)		0.8	0.5 (mhh) 0.17 (mlh)
Refractive index, n	2.2 (0.60 μm) 2.5 (0.23 μm)	2.35 (1.0 μm) 2.60 (0.38 μm)	2.56 (1.0 μm) 3.12 (0.66 μm)
ε (0)	9.14	10.4 (E‖c) 9.5 (E⊥c)	
ε (∞)	4.84	5.8 (E‖c) 5.4 (E⊥c)	9.3
Thermal conductivity, (κher/cm K)	2.0	1.7–1.8	
Melting point (°C)	2000	>1700	1100
ΔG^0 (kcal/mol)	−68.2	−33.0	−23.0
Heat capacity, C_p (cal/mol K)	7.6	9.7	10.0

Table 1. Physical properties of III–V nitride semiconductors [33].

3. Colloidal III–V nitride quantum dots

3.1. Syntheses of colloidal nitride quantum dots

So far, many efforts have been devoted to synthesize colloidal nitride quantum dots by the solution-phase routes. Over the past 20 years, many groups have prepared the colloidal III–V nitride quantum dots by various solution-based methods. These methods can be classified into the following approaches, namely solvothermal [24, 25, 34], hydrothermal [35], and thermal decomposition of single [36, 37] and two precursors [38]. The hydrothermal process refers to the reaction of reactants and water in a pressurized reaction environment to form nanoparticles. The process of forming of nanocrystals undergoes two stages, dissolution and crystallization. In the primary reaction, the aggregation and binding of the precursor particles are destroyed, making the particles dissolute in the hydrothermal solvent, transporting into the solution in the form of ions or ionic groups, and crystallizing the crystalline grain after nucleation. Solvothermal method was developed on the basis of hydrothermal method, which uses the organic solvent as solution, replacing water. In this way, some compounds sensitive to water (reacting with water, hydrolysis, resolution, or instability) like III–V group semiconductors, carbides, fluorides, and so on, can be prepared. LaMer and Dinegra thought that the preparation of monodisperse nanocluster needed a transient and discrete nucleation process, and then controlled the crystal nucleus growth slowly [39]. Putting the reactants rapidly into the container makes the precursor concentration higher than the nucleation threshold value. A short period of sudden

nucleation can reduce saturation. As long as the rate of the consuming concentration for nanocrystal growth reaction is less than the rate of precursor injection, there are no new nanocrystals formed. Therefore, the size of the particle distributions mostly depends on the time from nucleation to growth. This method has some advantages that cannot be replaced by other methods: (1) uniform morphology; (2) narrow size distribution; and (3) high crystallinity due to relatively high reaction temperature.

3.1.1. Gallium nitride

The preparation of colloidal GaN quantum dots via thermal decomposition commonly requires the suitable Ga and N resources as the precursors. As the growth temperature increases, the precursors will be decomposed rapidly, react, and then generate lots of small nanometal clusters. Finally, the GaN nanoparticles are formed after the further growth and the size of the particles depends on the reaction time and temperature. The precursor contains polymeric gallium imide [40, 41] and gallium cupferron with hexamethyldisilazane, [42] etc. The selection of the precursor is very important for successful growth of colloidal GaN quantum dots. Janik and Wells [41] prepared powders of mixed hexagonal/cubic nanocrystals of GaN by deamination of polymeric gallium imide ($\{Ga(NH)3/2\}_n$) at 210°C. Their work showed that nanosize GaN could be prepared by polymeric gallium imide ($\{Ga(NH)3/2\}_n$) at high temperature, due to the lack of any organic substituents in the precursor, which made $\{Ga(NH)3/2\}_n$ a good candidate for the generation of carbon-free GaN. However, it is unfortunate that these methods for the size control were limited and did not allow the nanocrystals to be dispersed in solvents to form transparent solutions of QDs suitable for optical measurements. One important factor in the synthesis of GaN is the purity of the final product. Carbon is usually left on QD surfaces after pyrolysis and it is difficult to remove. The elemental analyses of the GaN QDs showed 2.49–3.65% carbon content. Although the GaN QDs obtained by the above methods were of poor quality, it opened a window for researchers to find better ways to obtain the high-quality GaN QDs.

According to the previous reports, Mićić et al. [40] still used {Ga(NH)3/2}n to prepare the GaN but they added trioctylamine (TOA) and hexadecylamine (HDA) during the heating process. The HDA could improve hydrophobicity of the GaN surface because of its less sterical hinderance and much dense surface cap. Mićić also showed that TOA/HDA decreased carbon adsorption on the QD particles and after purification yields a white colloidal solution. A transmission electron microscopy (TEM) image of the GaN quantum dots is given in **Figure 1**, which shows the spherical GaN QDs with diameter ranging from 23 to 45 Å. High-resolution micrographs show <111> lattice fringes in some particles have the proper orientation for observing fringes (**Figure 1**, bottom right panels). The particle size was estimated by simply counting the lattice fringes for each particle (interplanar spacing for <111> GaN = 2.52 Å); and the average diameter is 30 Å ± 40%. The bottom left panel in **Figure 1** shows the electron diffraction pattern of the GaN nanocrystals.

The polymer is not a good solvent for controlling the size and the high-yield production of QDs. In the polymer solvent, during the nucleation process, due to the melt in the solvent, dispersibility is not good, the nanoclusters may be happened to aggregate. To solve this

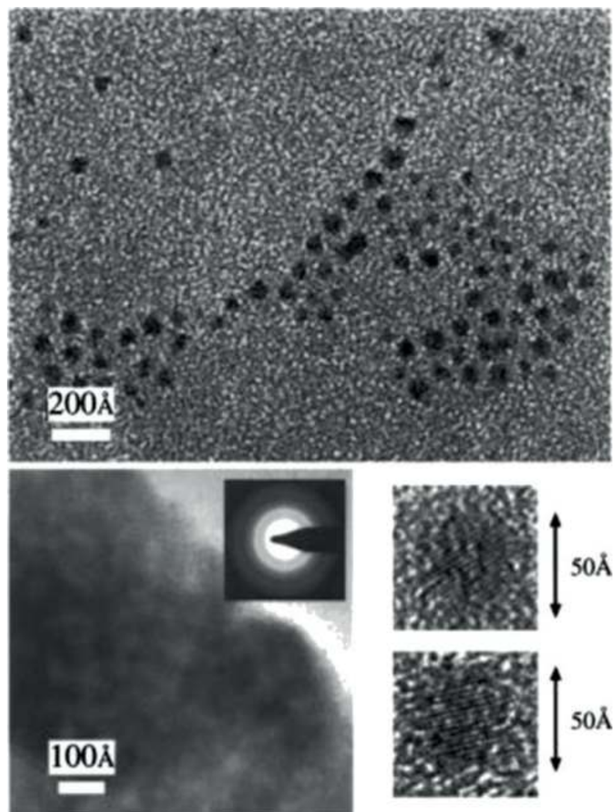

Figure 1. TEM image of GaN QDs taken in bright field. Top panel shows low magnification of QDs and some linear alignment. Bottom two right panels show high magnification and lattice fringes of QD oriented with the <111> axis in the plane of the micrograph. Bottom left panel shows electron diffraction pattern of GaN QDs indicating zinc-blende structure [40].

problem, Pan et al. [43] found that GaN could be obtained by dimeric amidogallium precursor ($Ga_2[N(CH_3)_2]_6$) through pyrolysis without the need for the polymeric intermediate. In this way, not only it produced colloidal GaN quantum dots, but also offered the possibilities of controlling the dots' size. In addition, the gaseous ammonia needed in the nucleation process was cancelled. Colloidal GaN QDs was got by transmission electron microscopy (TEM) imaging. **Figure 2** shows a TEM image of the GaN nanoparticles. Several spherical particles with diameters of 2–4 nm are shown in the **Figure 2**. Although the particle size distribution obtained here is not comparable with those obtained in the highly optimized II–VI group systems, it is believed that this reaction will be improved through optimizing the reaction conditions. However, the as-prepared samples' crystallinity is poor, which can be confirmed by the TEM images. No lattice fringes were observed in HRTEM images. HAD may has a contribution for the pyrolysis reaction. When HDA was eliminated from the reaction mixture,

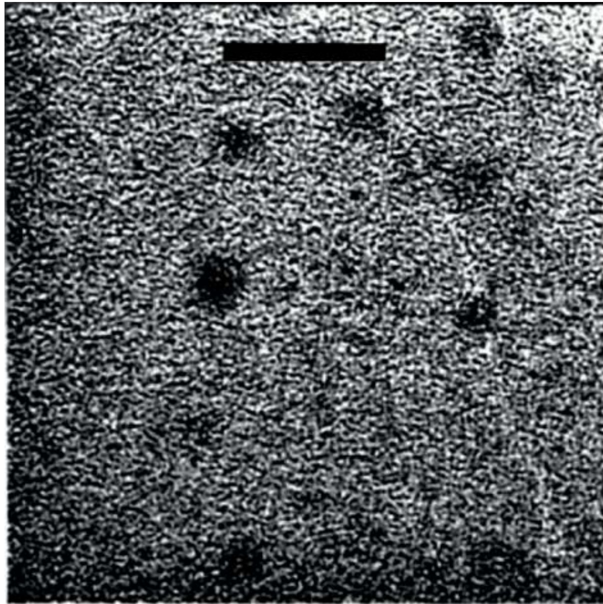

Figure 2. TEM image of GaN nanoparticles obtained from pyrolysis of $Ga_2[N(CH3)_2]_6$. Scale bar is 10 nm [43].

no GaN was produced. Elemental analysis on the GaN product prepared in the presence of HDA revealed a Ga/N mass ratio of 4.88:1 (theoretical 4.98:1), indicative of nearly stoichiometric GaN.

The sample also had a high-carbon content (C/N) of 2.27:1, indicating that carbon was incorporated into the particles. Certainly, it was consistent with capping of nanosize particles by capping ligands, such as HDA or TOA that contains long aliphatic chains.

Generally, to get the GaN, the post-treatment temperature is at least 500°C. Nitrides of lanthanide and transition metals (M) can be prepared by solid reaction at the temperature ranging from 600 to 1000°C. The chemical equation is as follows:

$$MCl_n + Li_3N \rightarrow MN + LiCl \quad (1)$$

Xie et al. [15] reported that the crystalline GaN particles could be synthesized by simple inorganic reactions at temperature of 300°C in the autoclave (no capping ligand in the whole preparation process). They used $GaCl_3$ and Li_3N as gallium and nitrogen precursors in the liquid, respectively, and the reaction equation is:

$$GaCl_3 + Li_3N \rightarrow GaN + 3LiCl \quad (2)$$

These crystallites of GaN have an average size of 32 nm and display a uniform shape (**Figure 3A**). The images of GaN particles were observed by High-resolution electron microscopy (HREM). In

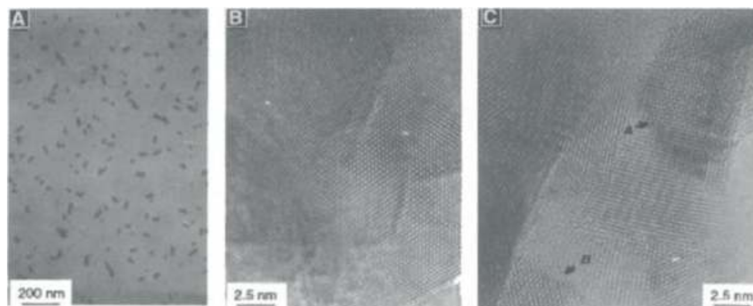

Figure 3. (A) A TEM micrograph of nanocrystalline GaN. (B and C) HREM images of nanocrystalline GaN: (B) lattice fringes of (001) plane in GaN with a wurtzite structure and (C) lattice fringes of (100) and (110) planes in GaN (marked A and B, respectively) with a rocksalt structure [15].

Figure 3B, the (001) lattice fringes of GaN in the wurtzite structure appear frequently, indicating the preferential orientation of the plate-like GaN particles. The areas marked by arrowheads (A and B) in **Figure 3C** represent a typical structural image of [100] and [110] orientations, respectively, of GaN in the rocksalt structure.

3.1.2. Indium nitride

Among the nitride, InN is the most unstable, which decomposes above 500°C [44]. Hence, it is difficult to prepare InN crystalline. Historically, polycrystalline indium nitride was synthesized by radio frequency sputtering [28], which results in high free-electron concentration, significant oxygen contamination, and an absorption edge at about 1.9 eV [45–47]. Recently, high-quality crystalline InN has been grown by molecular beam epitaxy (MBE) [27]. The typically observed bandgap of high-quality wurtzite-InN grown by MBE is around 0.65–0.7 eV [34, 48]. However, the quality of indium nitride samples grown by low-cost solution or other vapour methods has still remained challenging. Therefore, there still exists a huge challenge to synthesize high-quality InN nanocrystals using low-cost solution or vapour methods. So far, Xiao et al. [24] adopted the solvothermal using $NaNH_2$ and In_2S_3 as novel nitrogen and indium sources to prepare the indium nitride at 180–200 °C with the particle size ranging from 10 to 30 nm, and the reaction equation is:

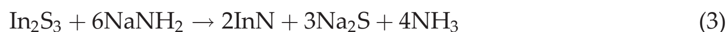

$$In_2S_3 + 6NaNH_2 \rightarrow 2InN + 3Na_2S + 4NH_3 \quad (3)$$

Hsieh [25] also used solvothermal to prepare the InN NCs with an average diameter of 6.2 ± 2.0 nm utilizing $InBr_3$ and $NaNH_2$ in a low temperature, ambient pressure, and liquid-phase condition.

Generally, ammonia is used as nitrogen source in the vapour-phase growth process. The relative high growth temperature in vapour-phase methods can help nucleation overcome the reaction difficulty encountered by solution methods. However, unlike the solution-based methods (where the nucleation and growth process could be separated by choosing appropriate ligands and solvents), the vapour-phase methods usually trigger off nonuniform nanocrystal

morphology due to poor control in the nucleation process. Moreover, the vapour-phase methods often encounter the aggregation problem due to the large surface energy of nanocrystals. It is concluded that each of the aforementioned methods for synthesis of monodisperse InN nanocrystals faces significant challenges in achieving well-defined size and shape. Our group [49] had addressed these critical issues by exploiting a new synthesis approach that resulted in monodisperse InN nanocrystals with uniform size and morphology and superior optical quality, and first successfully prepared the cubic InN nanocrystals with aforementioned advantages, by combining solution- and vapour-phase methods under silica shell confinement (SVSC), as schematically shown in **Figure 4(a)**.

In this method, the In_2O_3 nanocrystals with well-defined size and morphology were first synthesized by a solution-based method. The In_2O_3 nanocrystals were coated by silica shell before nitridation, this is because silica is inert and can be easily removed by HF acid. The obtained $In_2O_3@SiO_2$ nanopowders were put into a tube furnace. After being purged with NH_3 gas for 20 min, the furnace was heated to 500–700°C and kept for 5 h under NH_3 flow at 300 ml/min. Finally, large-scale $InN@SiO_2$nanocrystals with uniform size and morphology were obtained through the SVSC route. After removing the silica shell, InN NCs can be dispersed into DI water and then transferred to various nonpolar organic solvents by phase transfer, as shown in **Figures 4(b)** and **(c)**.

Figure 5(a) and **(b)** shows transmission electron microscopy (TEM) and high-resolution transmission electron microscopy (HRTEM) images of the InN nanocrystals. The indium nitride nanocrystals with nearly monodisperse spherical shape can be observed from the TEM images. The diameter distribution of the synthesized indium nitride nanocrystals can be revealed from the **Figure 5(c)**, revealing a fairly uniform size distribution of the InN nanocrystals from 5.0 to

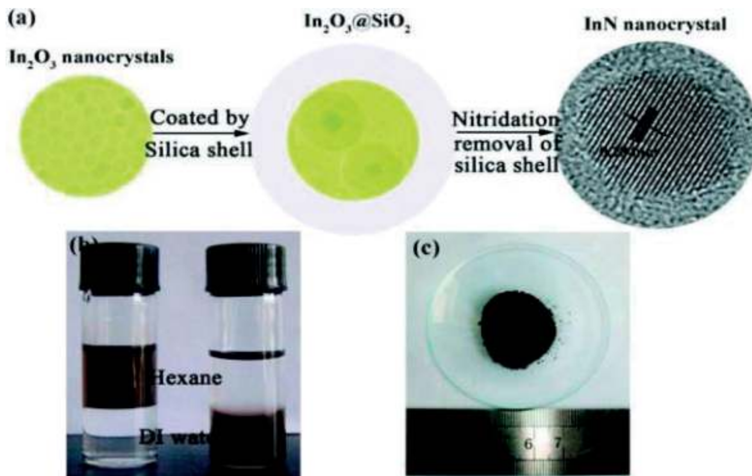

Figure 4. (a) Schematic of the SVSC method for InN nanocrystals. (b) The upper layer is hexane and the bottom layer is distilled water. The left bottle contains InN nanocrystals in hexane and the right one contains InN nanocrystals in water. (c) Large-scale $InN@SiO_2$ nanopowders (0.47 g) synthesized by the SVSC method [49].

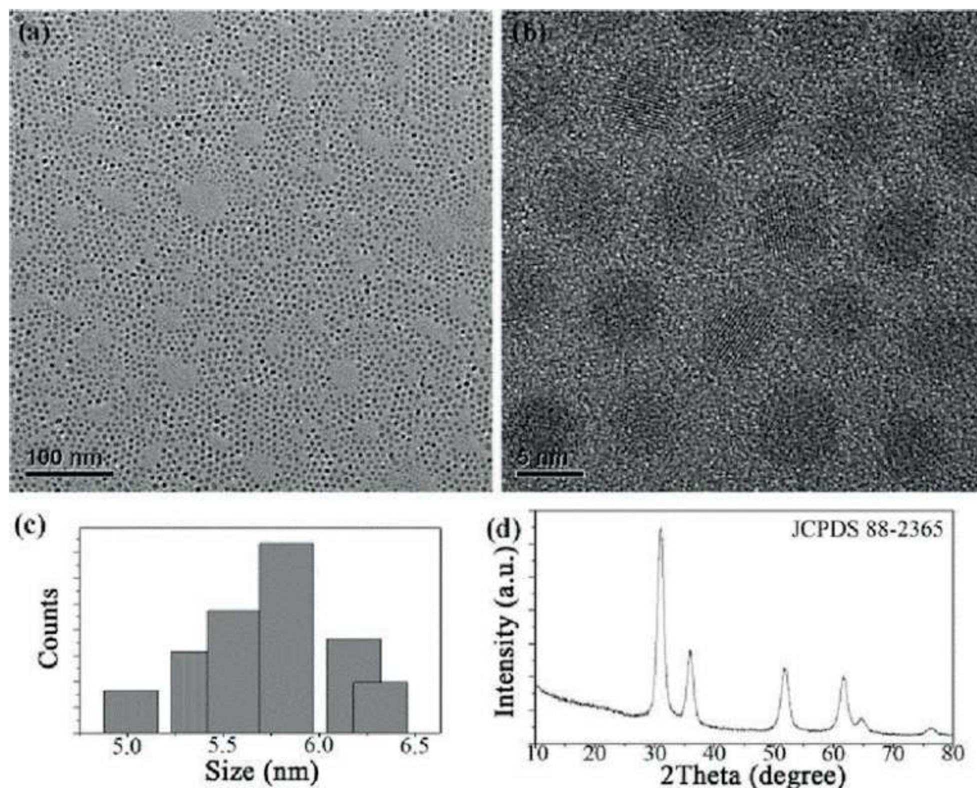

Figure 5. (a) Low-resolution TEM; (b) HRTEM images of the InN nanocrystals; (c) size distribution of the InN nanocrystals; and (d) XRD spectrum of the InN@SiO_2nanocrystals obtained at 550°C [49].

6.3 nm. The average diameter of the InN nanocrystals is calculated to be 5.7 $\pm$ 0.6 nm, after counting about 200 nanocrystals. **Figure 5d** shows the X-ray diffraction (XRD) pattern of the InN nanocrystals. All the peaks can be matched with the cubic InN (JCPDS No. 88-2365) except the peak at 2θ = 22.5°, which corresponds to the amorphous silica. No peaks of In_2O_3 were observed in the XRD pattern, indicating that all In_2O_3 nanocrystals had been converted to InN. As illustrated in **Figure 6**, the InN@SiO_2 nanocrystals in the form of powders (not in the solution) exhibited infrared PL at room temperature. The fluctuation of PL signal at ~1900 nm could be due to water absorption and might not originate from the sample. The PL spectrum is characterized by the presence of three distinct emission peaks.

3.1.3. Indium gallium nitride

Xiao et al. [50] demonstrated for the first time, a new route that quantum size effect can be used to prepare the epitaxial nanostructures with great significance for the achievement of a broad range of future nanoelectronic and nanophotonic devices. The process is quantum size-controlled photoelectrochemical (QSC-PEC) etching. Quantum dots' bandgap depends on the

http://dx.doi.org/10.5772/intechopen.70844

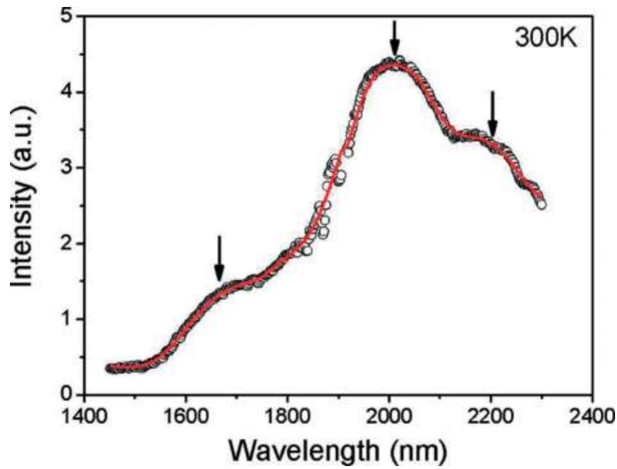

Figure 6. Photoluminescence spectrum of $InN@SiO_2$ nanocrystals at room temperature [49].

nanostructure size. Therefore, they used QSC-PEC etching to fabricate InGaN QDs of controlled size starting from the InGaN thin film. They used H_2SO_4 aqueous solution as the electrolyte and a tunable, relatively narrow band laser source as photoexcitation. The sample consisted of $In_{0.13}Ga_{0.87}N$ films (3–20 nm) grown on c-plane GaN/sapphire. They discussed the influence of solution pH during quantum size-controlled PEC etch process. [51] When the solution pH lies between 5 and 11, both Ga- and In-oxides are formed at the surface. Etching rates are very low and InGaN QDs are not formed. In the dark etching of InGaN at pH above 5, the above situation may also occur. However, when the solution pH is below 3, oxide-free QDs with self-terminated sizes can be successfully realized. In strongly acidic solutions, the oxides are not formed during the PEC etching process, due to all the oxide productions can be dissolved by the electrolyte. Therefore, PEC etching can be used to prepare InGaN QDs. Meanwhile, there are other methods of preparing InGaN quantum dot, such as plasma-assisted molecular beam epitaxy (PA-MBE) [30], metal-organic vapour phase epitaxy (MOVPE) [31], and metal-organic chemical vapour deposition (MOCVD) [32].

4. Summary and future directions

The field of colloidal III–V nitride quantum dots has been constantly gaining interest among science and engineering communities during the past decades. In this chapter, we have summarized the research status and progress in this field, including their preparation techniques and optoelectronic properties. Although much progress has already been made in the field of colloidal III–V nitride quantum dots, significant challenges involving the fabrication of quantum dots with uniform morphology and size and control of the electronic and optical properties in terms of composition and structure remain to be solved. Once high-quality colloidal III–V nitride quantum dots are synthesized successfully, more new discoveries and applications

will be exploited, such as solid-state lighting, lasing technologies, and optoelectronic devices, as well as the booming quantum photonics technology.

Acknowledgements

This work was financially supported by the National Natural Science Foundation of China (Grant No. 51472031, 51102017 and 21503014).

Author details

Zequn Chen[1], Chuli Sun[2], Wei Guo[2] and Zhuo Chen[1]*

*Address all correspondence to: zchen@bit.edu.cn

1 Department of Materials Physics and Chemistry, Beijing Key Laboratory of Construction Tailorable Advanced Functional Materials and Green Applications, School of Materials Science and Engineering, Beijing Institute of Technology Institution, Beijing, P.R. China

2 Department of Physics, Beijing Institute of Technology, Beijing, P.R. China

References

[1] Jie B, Moungi GB. A colloidal quantum dot spectrometer. Nature. 2015;**523**:67-70. DOI: 10.1038/nature14576

[2] Tang J, Sargent EH. Infrared colloidal quantum dots for photovoltaics: Fundamentals and recent progress. Advanced Materials. 2011;**23**:12-29. DOI: 10.1002/adma.201001491

[3] Yin Y, Alivisatos AP. Colloidal nanocrystal synthesis and the organic-inorganic interface. Nature. 2005;**437**:664-670. DOI: 10.1038/nature04165

[4] Colvin VL, Schlamp MC, Alivisatos AP. Light-emitteing-diodes made from cadmium selenide nanocrystals and a semiconducting polymer. Nature. 1994;**370**:354-357. DOI: 10. 1038/370354a0

[5] Jeong HK, Jae HL, Myeong JP, Seong HL, Kook HC, Chang HL. High-power genuine ultraviolet light-emitting diodes based on colloidal nanocrystal quantum dots. Nano Letters. 2015;**15**:3793-3799. DOI: 10.1021/acs.nanolett.5b00392

[6] Yu WW, Qu LH, Guo WZ, Peng XG. Experimental determination of the extinction coefficient of CdTe, CdSe, and CdS nanocrystals. Chemistry of Materials. 2003;**15**:2854-2860. DOI: 10.1021/cm034081k

[7] Moreels I, Lambert K, De Muynck D, Vanhaecke F, Poelman D, Martins JC, Allan G, Hens Z. Composition and size-dependent extinction coefficient of colloidal PbSe quantum dots. Chemistry of Materials. 2007;**19**:6101-6106. DOI: 10.1021/cm071410q

[8] Xia YN, Xiong YJ, Lim B, Skrabalak SE. Shape-controlled synthesis of metal nanocrystals: Simple chemistry meets complex physics. Angewandte Chemie International Edition. 2009;**48**:60-103. DOI: 10.1002/anie.200802248

[9] Puntes VF, Krishnan KM, Alivisatos AP. Colloidal nanocrystal shape and size control: The case of cobalt. Science. 2001;**291**:1019-1020. DOI: 10.1126/science.1057553

[10] Reiss P, Carriere M, Lincheneau C, Vaure L, Tamang S. Synthesis of semiconductor nanocrystals, focusing on nontoxic and earth-abundant materials. Chemical Review. 2016;**116**:10731-10819. DOI: 10.1021/acs.chemrev.6b00116

[11] Nakamura S, Pearton SJ, Fasol G. The Blue Laser Diode: The Complete Story. 2nd ed. New York: Springer-Verlag; 2000. 104 p. DOI: 10.1007/978-3-662-04156-7

[12] Wu Y, Jacob-mitos M, Moore ML, Heikman S. A 97.8% efficient GaN HEMT boost converter with 300-W output power at 1 MHz. IEEE Electron Device Letters. 2008;**29**:824-826. DOI: 10.1109/LED.2008.2000921

[13] Nakamura S, Faso G. The Blue Laser Diode. The Complete Story. Berlin: Springer; 1999. 72 p. DOI: 10.1007/978-3-662-04156-7

[14] Kocha SS, Peterson MW, Arent DJ, Redwing JM, Tischler MA, Turner JA. Electrochemical investigation of the gallium nitride-aqueous electrolyte interface. Journal of the Electrochemical Society. 1995;**142**:L238-L240. DOI: 10.1149/1.2048511

[15] Xie Y, Qian Y, Wang W, Zhang S, Zhang Y. A benzene-thermal synthetic route to nanocrystalline GaN. Science. 1996;**272**:1926-1927. DOI: 10.1126/science.272.5270.1926

[16] Guo Q, Kato O, Yoshida A. Thermal stability of indium nitride single crystal films. Journal of Applied Physics. 1993;**73**:7969-7971. DOI: 10.1063/1.353906

[17] Yasushi N, Yoshiki S, Tomohiro Y. RF-molecular beam epitaxy growth and properties of InN and related alloys. The Japan Society of Applied Physics. 2003;**42**:2549-2559. DOI: 10.1143/JJAP.42.2549

[18] Faso GS, Nakamura S. The Blue Laser Diode: GaN Based Light Emitters and Lasers. Berlin, Hong Kong: Springer; 1997. 15 p. DOI: 10.1007/978-3-662-03462-0

[19] Starikov E, Shiktorov P, Gruninskis V. Monte Carlo calculations of THz generation in wide gap semiconductors. Physica B. 2002;**341**:171-175. DOI: 10.1016/S0921-4526(01)01374-6

[20] Neff H, Semchinova OK, AMN L, Filimonov A, Holzhueter G. Photovoltaic properties and technological aspectsof $In_{1-x}Ga_xN$/Si, Ge ($0 < x < 0.6$) heterojunction solar cells. Solar Energy Materials & Solar Cells. 2006;**90**:982-997. DOI: 10.1016/j.solmat.2005.06.002

[21] Nguyen HPT, Chang Y-L, et al. InN p-i-n nanowire solar cells on Si. IEEE Journal of Selected Topics in Quantum Electronics. 2011;**17**:1062-1069. DOI: 10.1109/JSTQE.2010.2082505

[22] Wu JQ. When group-III nitrides go infrared: New properties and perspectives. Journal of Applied Physics. 2009;**106**:011101-011128. DOI: 10.1063/1.3155798

[23] Michalet X, Pinaud FF, Bentolila LA, et al. Quantum dots for live cells, in vivo imaging, and diagnostics. Science. 2005;**307**:538-544. DOI: 10.1126/science.1104274

[24] Xiao J, Xie Y, Tang R, Luo W. Benzene thermal conversion to nanocrystalline indium nitride from sulfide at low temperature. Inorganic Chemistry. 2003;**42**:107-111. DOI: 10.1021/ic0258330

[25] Hsieh JC, Yun DS, Hu E, Belcher AM. Ambient pressure, low-temperature synthesis and characterization of colloidal InN nanocrystals. Journal of Materials Chemistry. 2010; **20**:1435-1437. DOI: 10.1039/b922196d

[26] Hovel HJ, Cuomo JJ. Electrical and optical properties of rf-sputtered GaN and InN. Applied Physics Letters. 1972;**20**:71-73. DOI: 10.1063/1.1654051

[27] Chang Y-L, Mi Z, Li F. Photoluminescence properties of a nearly intrinsic single InN nanowire. Advanced Functional Materials. 2010;**20**:4146-4151. DOI: 10.1002/adfm.201000739

[28] Moses PG, Van de Walle CG. Band bowing and band alignment in InGaN alloys. Applied Physica Letters. 2010;**96**:021908-021910. DOI: 10.1063/1.3291055

[29] Nakamura S. The roles of structural imperfections in InGaN-based blue light-emitting diodes and laser diodes. Science. 1998;**281**:956-961. DOI: 10.1126/science.281.5379.956

[30] Deshpande S, Frost T, Yan LF, et al. Formation and nature of InGaN quantum dots in GaN nanowires. Nano Letters. 2015;**15**:1647-1653. DOI: 10.1021/nl5041989

[31] Tsai HL, Wang TY, Yang JR, et al. Observation of ultrahigh density InGaN quantum dots. Journal of Applied Physics. 2007;**102**:013521-013524. DOI: 10.1063/1.2745848

[32] Zhang L, Teng C-H, Hill TA, et al. Single photon emission from site-controlled InGaN/GaN quantum dots. Applied Physica Letters. 2013;**103**:192114-192118. DOI: 10.1063/1.4830000

[33] Mohamed H, Razeghi M. Optoelectronic Devices: III Nitrides. United Kingdom: Elsevier; 2005. 59 p. DOI: 10.1016/B978-008044426-0/50000-6

[34] Sardar K, Deepak FL, Govindaraj A, Seikh MM, Rao CN. InN nanocrystals, nanowires, and nanotubes. Small. 2005;**1**:91-94. DOI: 10.1002/smll.200400011

[35] Xiong Y, Xie Y, Li Z, Li X, Zhang R. Aqueous synthesis of group IIIA nitrides at low temperature. New Journal of Chemistry. 2004;**28**:214-217. DOI: 10.1039/b310373k

[36] Frank AC, Stowasser F, et al. Detonations of gallium azides: A simple route to hexagonal GaN nanocrystals. Journal of American Chemical Society. 1998;**120**:3512-3513. DOI: 10.1002/chin.199828028

[37] Sardar K, Dan M, et al. A simple single-source precursor route to the nanostructures of AlN, GaN and InN. Journal of Materials Chemistry. 2005;**15**:2175-2177. DOI: 10.1039/b502887f

[38] Chen C, Liang C. Syntheses of soluble GaN nanocrystals by a solution-phase reaction. Tamkang Journal of Science and Engineering. 2002;**5**:223-226

[39] Lamer VK, Dingar RH. Theory, production and mechanism of formation of monodispersed hydrosols. Journal of American Chemical Society. 1950;**72**:4847-4854. DOI: 10.1021/ja01167a001

[40] Mićić OI, Ahrenkiel SP, Bertram D, Nozik AJ. Synthesis, structure, and optical properties of colloidal GaN quantum dots. Applied Physics Letters. 1999;**75**:478-480. DOI: 10.1063/1.124414

[41] Janik JF, Wells RL. Gallium imide, $\{Ga(NH)_{3/2}\}_n$, a new polymeric precursor for gallium nitride powders. Chemistry of Materials. 1996;**8**:2708-2711. DOI: 10.1002/chin.199710018

[42] Sardar K, Rao CNR. New solvotherma routes for GaN nanocrystals. Advanced Materials. 2004;**16**:425-429. DOI: 10.1002/adma.200306050

[43] Pan GQ, Kordesch ME, Patten PGV. New pyrolysis route to GaN quantum dots. Chemistry of Materials. 2006;**18**:3915-3917. DOI: 10.1021/cm060368g

[44] Tranior JW, Rose K. Some properties of InN films prepared by reactive evaporation. Journal of Electronic Materials. 1974;**3**:821-828. DOI: 10.1007/BF02651400

[45] Westra KL, Lawson RPW, Brett MJJ. The effects of oxygen contamination on the properties of reactively sputtered indium nitride films. Journal of Vacuum Science & Technology A. 1998;**6**:1730-1732. DOI: 10.1116/1.575280

[46] Tansley TL, Foley CP. Optical band gap of indium nitride. Journal of Applied Physics. 1986;**59**:3241-3244. DOI: 10.1063/1.336906

[47] Morkoc H. Nitride Semiconductors and Devices. Heidelberg: Springer; 1999. 32 p. DOI: 10.1007/978-3-642-58562-3

[48] Cesar M, Ke YQ, Ji W, Guo H, Mi ZT. Band gap of $In_xGa_{1-x}N$: A first principles analysis. Applied Physics Letters. 2011;**98**:202107-202109. DOI: 10.1063/1.3592573

[49] Chen Z, Li YN, Cao CB, et al. Large-scale cubic InN nanocrystals by a combined solution- and vapor-phase method under silica confinement. Journal of American Chemical Society. 2012;**134**:780-783. DOI: 10.1021/ja209072v

[50] Xiao XY, Fischer AJ, Wang GT, et al. Quantum-size-controlled photoelectrochemical fabrication of epitaxial InGaN quantum dots. Nano Letters. 2014;**14**:5616-5620. DOI: 10.1021/nl502151k

[51] Xiao XY, Lu P, et al. Influence of pH on the quantum-size-controlled photoelectrochemical etching of epitaxial InGaN quantum dots. The Journal of Physical Chemistry C. 2015;**119**:28194-28198. DOI: 10.1021/acs.jpcc.5b09555